A novel identification procedure from ambient vibration data for buildings of the cultural heritage

Cristiano Bilello[a], Alberto Di Matteo[b], Annalisa Fersini[b], Chiara Masnata[b], Antonina Pirrotta[b,c], Salvatore Russotto[b]
[a] *ABGroup s.n.c Ingegneria e Servizi Tecnici integrati, Sciacca, Italy*
[b] *Dipartimento di Ingegneria, University of Palermo, Palermo, Italy*
[c] *Department of Mathematical Sciences, University of Liverpool, Liverpool, UK*

Keywords: Operational Modal Analysis, Hilbert Transform, Analytical signal

ABSTRACT
Ambient modal identification, also known as Operational Modal Analysis (OMA), aims to identify the modal properties of a structure based on vibration data collected when the structure is under its operating conditions, i.e., no initial excitation or known artificial excitation. This procedure for testing and/or monitoring historic buildings, is particularly attractive for civil engineers concerned with the safety of complex historic structures. However, since the external force is not recorded, the identification methods have to be more sophisticated and based on stochastic mechanics.
In this context, this contribution will introduce an innovative ambient identification method based on applying the Hilbert Transform, to obtain the analytical representation of the system response in terms of the correlation function. In particular, it is worth stressing that the analytical signal is a complex representation of a time domain signal: the real part is the time domain signal itself, while the imaginary part is its Hilbert transform. A real historic building has been considered as a case study, Chiaramonte Palace, and results assess the efficiency of the proposed method. Chiaramonte Palace, known as "Steri", is a rare and precious example of fourteenth-century architecture in Sicily. It is located in the "Marina", a hinge between the harbor of the city of Palermo and part of the ancient quarter of Kalsa, and today it is the headquarters of the University's Rector.

1 INTRODUCTION

The accurate estimation of the modal parameters (frequencies, damping coefficients and mode shapes) of a structure has become a challenging phase in the structural analysis to preserve historical and monumental heritage from seismic actions.

The identification of the dynamic characteristics is fundamental in order to investigate the seismic vulnerability of existing structures, to plan enhancing changes, to update structural models as well as setting up vibration-based structural health monitoring.

In the past, the modal identification was generally based on force vibration tests involving impacts tests or other complex setups applying several types of input exciters directly in-situ.

In this context, it is customary to refer to the modal analysis based on artificial forced excitation as Experimental Modal Analysis (EMA) which presupposes the use of both known input and structural response measurements to estimate modal parameters.

Nowadays, the current trend in the modal identification field suggests the use of another technique, the Operational Modal Analysis (OMA), also named as ambient or output-only modal analysis (Brincker et al. 2005).

OMA is denoted as an ambient vibration identification method since it allows dynamic tests to be performed in in-service structures, considered not subjected to artificial forces but to ambient noise vibrations (wind, traffic, water waves, man-made excitations and so on). Hence, the modal identification associated with OMA techniques requires to recorder response data only without the need to know the input force.

Tackling issues involved in the measure of dynamic forces exciting structures, OMA is of-ten preferable in the structural health monitoring field compared to classical EMA tests, which normally

may not be conducted routinely and economically since they interfere with the operating condition of structures.

In the framework of OMA, researchers have demonstrated the reliability of both frequency and time domain approaches to estimate the structural modal parameters of a large variety of structures (Brincker et al. 2005). It is worth noting that, since the external force is not recorded, testing OMA procedures are based on concepts from stochastic mechanics (Barone et al. 2008).

Classical OMA frequency domain techniques generally extract the modal parameters from the frequency response functions (FRFs) or from the auto power spectral density functions (PSDs) and cross power spectral density functions (CPSDs) of the outputs, considering that modes can be estimated taking into ac-count the amplitude of their peaks at the correspondent main frequencies of the system (Bendat and Piersol 1993).

Among the several OMA procedures, the main and most utilized are the Peak-picking combined with the Half power (PP+HP) (Bendat and Piersol 2011) and the Frequency Domain Decomposition (FDD) (Brincker et al. 2000). These methods are generally based on the input-output PSD relationship (Bendat and Piersol 2011). Clearly, in this case, the PSD of the input is unknown since the excitation source is due to natural or operative loadings. Thus, the basic idea of OMA hypotheses a white noise process as external force, characterized by a flat power spectral density in the frequency range of interest (Brincker et al. 2000). Hence, under white noise assumption, all the FRFs and PSDs/CPSDs of the output are known in the frequency domain. It is worth highlighting that then, by using the Wiener–Khinchine theorem (Bendat and Piersol 2011), the auto correlation functions (CORs) and cross correlation functions (CCORs) of the output can be obtained in the time domain too.

As it is well known, since frequency domain-based methods depend strongly on the frequency resolution of the FRFs/PSDs, the identified modal parameters, and especially the damping estimation could not be very accurate when the damping is very high or the modes are very close to each other (Bendat and Piersol 2011).

In the present study, an identification technique, focused on the identification of the damping ratio and based on applying the Hilbert Transform (HT) (Cottone et al. 2008), (Cottone et al. 2014), (Lo Iacono et al. 2012), to obtain the analytical signal (AS) in terms of correlation functions, has been developed. Notably, the analytical signal is a complex representation of a time domain signal: the real part is the time domain signal itself, while the imaginary part is its Hilbert transform. It has been observed that it is very vulnerable to variations of some signal quantities, such as phase and instantaneous frequency, so it seems to be an appealing means to detect with high precision the modal parameters of a structure (Agneni 2004).

Moreover, AS is combined with a proper mode decomposition algorithm which, assuming a stationary white noise process as external force, decomposes the initial output PSD matrix in a summation of monocomponent "filtered" PSDs/CPSDS, each one corresponding to a single oscillator (Cottone et al. 2008). Then, once the FPSDs/FCPSDs are transformed into monocomponent CORs/CCORs of the outputs, the structural parameters can be detected in the time domain.

In this contribution, the identification algorithm is presented for a single degree of freedom (SDOF) system and a numerical analysis carried out on the Chiaramonte Palace, a real historic building located in Palermo and known as "Steri", proves the efficiency of the proposed method.

2 IDENTIFICATION ALGORITHM

In this paper, an innovative ambient identification method to estimate the frequencies and the damping ratios of a structure from the analytical signal of the output vibration data is proposed. Once the output signals of a system, subjected to environmental noise, have been acquired in terms of accelerometer data, it is necessary to estimate the PSDs/CPSDs in the frequency domain in order to obtain the CORs/CCORs. Finally, by means of the Hilbert Transform (HT), it is possible to define the analytical signal (AS), a complex signal which allows the dynamic characteristics (frequencies, damping coefficients) to be easily extracted from its properties.

The method, denoted as Analytical Signal-based method (ASM), can be summarized in the following steps:

1) Acquisition of the structural response signals;
2) Estimation of the PSDs/CPSDs from output data (Welch method);
3) Estimation of the CORs/CCORs from the PSDs/CPSDs (Wiener-Kinchine), by means of the inverse fast Fourier transform (IFFT);
4) Estimation of the AS (by means of the HT) and its properties (Envelope, phase);

5) Identification of the modal parameters (instantaneous frequencies and damping ratios).

The meaning of each step will be explained in detail in the following example resorting a linear SDOF structural model (Figure 1).

Consider a structural system with mass M_1, stiffness K_1 and damping C_1, set so that the value of the damping ratio $\zeta_1 = C_1 / \left(2\sqrt{K_1 M_1}\right)$ is 0.05 and the natural frequency $f_1 = \sqrt{K_1 / M_1} / (2\pi)$ is 30 Hz. These two parameters represent the modal properties to be identified with the proposed procedure.

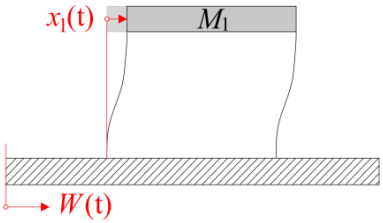

Figure 1. SDOF structural model.

The system is excited by a white noise process $W(t)$ as the external force so that the power spectrum of the input is flat. Let $x_1(t)$ denote the displacement response of the SDOF system relative to the ground. The dynamic behavior of this system is governed by the following equation of motion:

$$\ddot{x}_1(t) + 2\zeta_1 \dot{x}_1(t) + \omega_1^2 x_1(t) = W(t) \qquad (1)$$

where $\omega_1 = 2\pi f_1$ is the circular frequency.

In order to estimate the output in terms of PSD, the Welch Method (Welch 1967) is applied to the structural acceleration $\ddot{x}_1(t)$ (Figure 2).

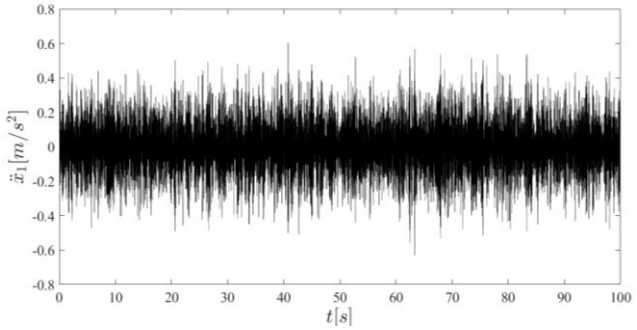

Figure 2: Structural acceleration.

Specifically, the application of the Welch Method requires some parameters such as the window function (Hanning, Hamming, etc...), the sub-segments length and the percentage of overlap to be set (Barbé et al. 2010). As a matter of fact, the original signal $\ddot{x}_1(t)$ is divided into $\bar{N}$ sub-segments, overlapped in time. To each one a window function is applied in the time domain so that the sub-signal tends to zero at the edges. In this numerical example, the Hamming window, an overlap of 50% between adjacent segments and a sample rate of 1000 Hz have been applied.

Then, by means of the Fast Fourier Transform (FFT), computed for each sub-signal, the two-sided PSD of each sub-signal, denoted as $S_{\ddot{x}_1\ddot{x}_1,r}(f)$, (with $r = 1,2 \ldots \bar{N}$) can be obtained by:

$$S_{\ddot{x}_1\ddot{x}_1,r}(f) = \frac{1}{2\pi} lim_{T\to\infty} \frac{1}{2T} E[\left|X_{1,r}(f)\right|^2] \qquad (2)$$

where $X_{1,r}(f)$ is the Fourier transform of each sub-signal of $\ddot{x}_1(t)$.

The mean of all the "sub" PSDs gives the total two-sided PSD function $S_{\ddot{x}_1\ddot{x}_1}(f)$ of the structural acceleration $\ddot{x}_1(t)$ (Figure 3):

$$S_{\ddot{x}_1\ddot{x}_1}(f) = \frac{1}{\bar{N}} \sum_{r=1}^{\bar{N}} S_{\ddot{x}_1\ddot{x}_1,r}(f) \qquad (3)$$

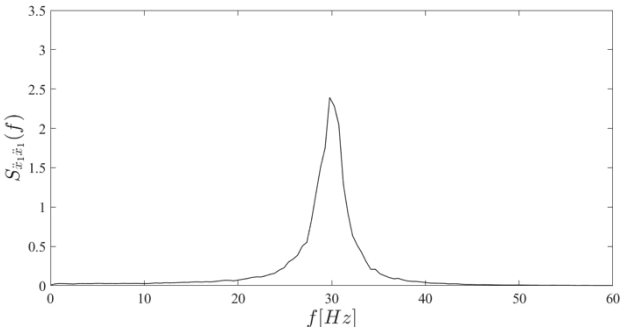

Figure 3: PSD function of the structural acceleration response.

According to the Wiener–Khinchine theorem, the IFFT of the $S_{\ddot{x}_1\ddot{x}_1}(f)$ yields the corresponding correlation function $R_{\ddot{x}_1\ddot{x}_1}(\tau)$ (Figure 4):

$$R_{\ddot{x}_1\ddot{x}_1}(\tau) = \int_{-\infty}^{+\infty} S_{\ddot{x}_1\ddot{x}_1}(f) e^{i2\pi f\tau} d\omega \qquad (4)$$

where i is the imaginary unit.

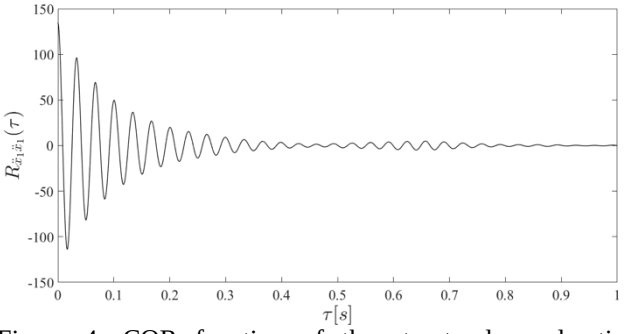

Figure 4: COR function of the structural acceleration response.

At this point, the Hilbert transform operator can be straightforwardly applied to the correlation function. Its HT is defined as:

$$\hat{R}_{\ddot{x}_1\ddot{x}_1}(\tau) = \frac{1}{\pi}\wp\int_{-\infty}^{\infty}\frac{R_{\ddot{x}_1\ddot{x}_1}(\tau)}{\mathrm{t}-\tau}\,\mathrm{d}\tau \tag{5}$$

where $\wp$ stands for the principal value.

The complex analytical signal $z_{\ddot{x}_1\ddot{x}_1}(\tau)$, in terms of the correlation function, is defined as:

$$z_{\ddot{x}_1\ddot{x}_1}(\tau) = R_{\ddot{x}_1\ddot{x}_1}(\tau) + i\hat{R}_{\ddot{x}_1\ddot{x}_1}(\tau) \tag{6}$$

The AS is a complex representation of a time domain signal. Specifically, in this case, the real part is the correlation function itself $R_{\ddot{x}_1\ddot{x}_1}(\tau)$, while the imaginary part is its Hilbert transform $\hat{R}_{\ddot{x}_1\ddot{x}_1}(\tau)$ (Figure 5).

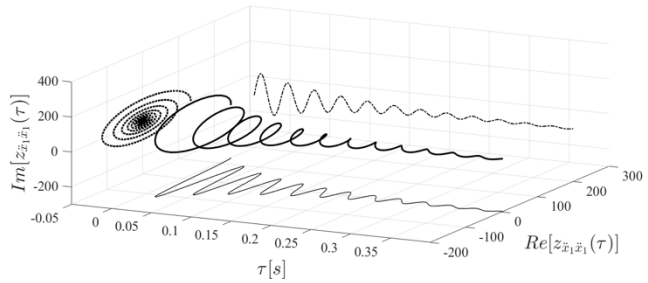

Figure 5: Analytical signal: complex representation of a time domain signal (AS-black thick line; real part-black line; imaginary part-dashed dotted black line; phase diagram-dotted black line).

The two main properties characterizing the analytical signal are the amplitude (or envelope) $\mathrm{A}_1(\tau)$ and the phase angle $\theta_1(\tau)$, respectively defined as:

$$\mathrm{A}_1(\tau) = \sqrt{R_{\ddot{x}_1\ddot{x}_1}(\tau)^2 + \hat{R}_{\ddot{x}_1\ddot{x}_1}(\tau)^2} \tag{7}$$

$$\theta_1(\tau) = \arctan\left[\frac{\hat{R}_{\ddot{x}_1\ddot{x}_1}(\tau)}{R_{\ddot{x}_1\ddot{x}_1}(\tau)}\right] \tag{8}$$

These two functions allow the damping ratio and the main frequency of the system to be derived. In particular, from the phase angle $\theta_1(\tau)$ is possible to extract the structural frequency while from the amplitude the damping ratio. According to (Agneni 2004) and considering the Bedrosian theorem (Bedrosian 1962), (Bedrosian 1963), the correlation function and its Hilbert transform can be expressed in the form:

$$R_{\ddot{x}_1\ddot{x}_1}(\tau) = -E_1\, e^{-2\pi f_1\xi_1\tau}\sin\left(2\pi\bar{f}_1\tau+\phi_1\right) \tag{9}$$

$$\hat{R}_{\ddot{x}_1\ddot{x}_1}(\tau) = -E_1\, e^{-2\pi f_1\xi_1\tau}\cos\left(2\pi\bar{f}_1\tau+\phi_1\right) \tag{10}$$

where E_1 is a constant, $\bar{f}_1 = f_1\sqrt{1-\zeta_1^2}$ the natural damped frequency of the system and ϕ_1 the initial phase.

In the light of above, the amplitude $\mathrm{A}_1(\tau)$ and the phase angle $\theta_1(\tau)$ of the analytical signal assume the following expressions:

$$\mathrm{A}_1(\tau) = E_1\, \mathrm{e}^{-2\pi \mathrm{f}_1\xi_1\tau} \tag{11}$$

$$\theta_1(\tau) = 2\pi\bar{f}_1\tau + \phi_1 \tag{12}$$

Although the frequency is known from the PSD analysis and it could be identified by the use of the PP method, it is worth noting that the first derivative of the phase angle $\theta_1(\tau)$ (considered as an unwrapped function as discussed in (Lo Iacono at al. 2012) yields a time dependent function, termed instantaneous frequency:

$$\bar{f}_{1,ist}(\tau) = \frac{\dot{\theta}_1(\tau)}{2\pi} \tag{13}$$

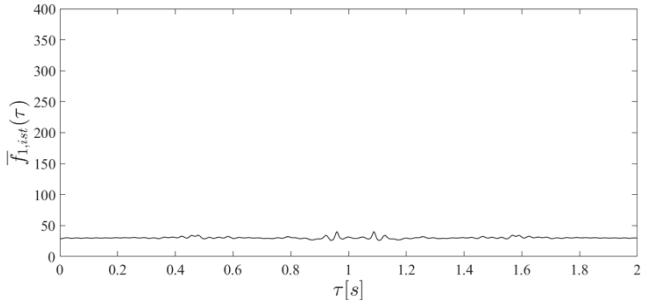

Figure 6: Instantaneous frequency function.

As it can be seen in Figure 6, the $\bar{f}_{1,ist}(\tau)$ is an almost constant function, so the natural damped frequency of the system $\bar{f}_1$ can be identified as its mean value:

$$\bar{f}_1 = E[\,\bar{f}_{1,ist}(\tau)] \tag{14}$$

with $E[\cdot]$ denoting the expectation operator.

Further, from the logarithmic representation of the amplitude, depicted in Figure 7, the damping ratio can be derived.

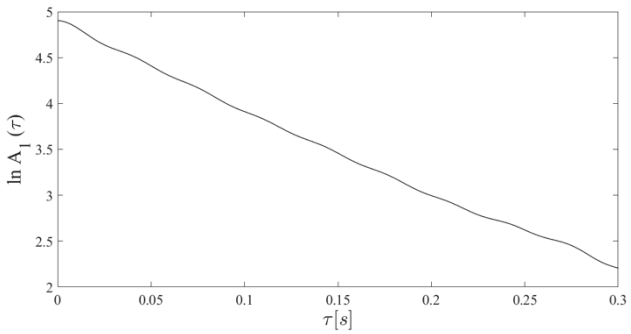

Figure 7: Logarithmic representation of the amplitude of the analytical signal.

Note that the natural logarithm of the amplitude defined in Eq. (11) can be represented by a straight line of coefficients c_1 and c_2 as follows:

$$\ln(\mathrm{A}_1(\tau)) = \ln E_1 - 2\pi f_1 \zeta_1 \tau = c_1 \tau + c_2 \qquad (15)$$

Consequently, the damping ratio ζ_1, associated with the instantaneous frequency f_1, is given by the relationship between the tangent to the logarithmic representation of $\mathrm{A}_1(\tau)$ and the frequency:

$$\zeta_1 = \frac{\tan[\ln \mathrm{A}_1(\tau)]}{2\pi f_1} \qquad (16)$$

Table 1 shows the natural damped frequency and the damping ratio estimated by the ASM and PP+HP and the discrepancies computed with respect to the exact values ($\overline{f}_1 = 29.9625$ Hz, $\zeta_1 = 0.0500$). As emerges, results are similar by employing both methods. In particular, the ASM attains slightly more accurate estimates compared to PP+HP. Importantly, the small differences occurring between exact and identified values, computed for both the modal parameters, prove as the aforementioned approach can be considered as a reliable output data-based tool for the estimation of modal parameters.

Table 1. Estimated natural frequency and damping ratio for $\zeta_1 = 0.05$ (exact value).

	PP+HP	Discrepancy [%]	ASM	Discrepancy [%]
$\overline{f}_1$ [Hz]	30.2365	0.9144	29.9100	0.1753
ζ_1	0.0494	1.1786	0.0499	0.2490

Finally, the analysis has been carried out increasing the damping ratio of the system. Indeed, it has been demonstrated that the estimation of modal parameters, and especially of the damping coefficient, based on methods which presuppose the knowledge of auto and cross-spectra of the output (such as PP+HP and FDD), it is reliable if some conditions are respected (Bendat and Piersol 2011). Specifically, a limit imposing that the damping ratio should be lower than 0.05.

Therefore, in order to investigate the capability of the ASM to overcome limits involved in frequency domain-methods, the damping ratio of the system has been increased so that $\zeta_1 = 0.08$.

The obtained values and discrepancies on the identification of frequency and damping ratio are reported in Table 2:

Table 2. Estimated natural frequency and damping ratio for $\zeta_1 = 0.08$ (exact value).

	PP+HP	Discrepancy [%]	ASM	Discrepancy [%]
$\overline{f}_1$ [Hz]	30.1819	0.9298	29.6018	1.0101
ζ_1	0.0777	2.8786	0.0789	1.3928

As shown in Table 2, using both the PP+HP and the ASM methods, the natural damped frequency is still well estimated, whereas looking at the considered higher damping ratio, as it is expected, the ASM can achieve a better estimation. This result suggests that the ASM, overcoming the limitations involved in frequency domain-based methods, can be adopted as a reliable identification method even when dealing with structures characterized by damping ratios greater than the 5%.

It is worth noting that, dealing with a multi degree of freedom (MDOF) system, although the procedure is the same as that described for the SDOF system, the steps have to take into account that the initial PSD matrix of the response data contains multicomponent PSDs/CPSDs characterized by the contribution of all the modes for each degree of freedom.

As a matter of fact, as well-known from modal analysis, for a MDOF system with n degrees of freedom, the generic displacement response $x_j(t)$ (with $j = 1, 2, .., n$) is the sum of the modal responses:

$$x_j(t) = \sum_{p=1}^{n} \phi_{jp} q_p(t) = \sum_{p=1}^{n} x_{jp}(t) \qquad (17)$$

where p indicates the mode and ϕ_{jp} is the jpth element of the system modal matrix and $q_p(t)$ the displacement in the modal space.

From the superposition formula it emerges that the response $x_j(t)$ of each degree of freedom j is influenced by all the structural modes ϕ_{jp}.

Consequently, also the responses in terms of PSDs/CPSDs will contain the contribution of all the modes. In this case, the modal parameters cannot be extracted directly from the derived analytical signals in the time domain.

In order to apply the proposed method, PSDs/CPSDs should be decomposed in such a way that monocomponent signals corresponding to several SDOF systems, each one containing information about a specific structural mode, are obtained.

It worth stressing that the decomposition into monocomponent PSDs/CPSDs, herein denoted as "filtered" PSDs (FPSDs) and filtered CPSDs (FCPSDs), can be achieved by means of proper filters (such as the Butterworth filter for instance). Once FPSDs/FCPSD are estimated, the correspondent filtered auto correlation functions (FCORs) and filtered cross correlation functions (FCCORs) can be obtained and the method is exactly applicable to each filtered function as shown for the SDOF system.

3 A CASE STUDY: CHIARAMONTE PALACE IN PALERMO

A practical implementation of the proposed procedure, applied to a real case study, is here presented and results have been compared with those achieved by applying the PP+HP.

The building considered in this paper is the Chiaramonte Palace, located in Palermo (Italy). This imposing fortress-palace, also known as "Lo Steri", (from "hosterium", meaning a fortified place), is in the city area called "Marina", a hinge between the harbour and part of the ancient Arabic quarter named Kalsa (Figure 8). The palace is a three-floor masonry structure built in the 1307 by the will of Giovanni Chiaramonte the "Old", member of the most powerful and influent family of that time (Lima 2006).

It represents a rare and precious example of XIV-century Sicilian architectural style showing Arabics and Normans influences. Its role as a symbol of the royal power in Sicily justifies its dimensions and peculiarities: its squared floor plans, gravitating on a porticoed courtyard, hold broad delegation rooms for public assemblies. The palace went through many changes and restorations and it was used for different scopes since the fifteenth century. Many spaces were converted into and offices, exhibition areas and museums (Giuffrè 2008) and currently it houses the rectorate of the University of Palermo.

Figure 8. Satellite view of Chiaramonte Palace in Palermo.

The palace square plan, with a side of about 40 meters, consists of four wings surrounding the magnificent courtyard with its portico on the ground floor and the upper loggia, anticipating the Renaissance model of a mansion.

The courtyard (Figure 9) is the main architectural element of the building and it is the object of the present study. The magnificent dual arcade, surmounted by a terrace, presents essential shapes with ogival arches resting on columns with capitals of different appearance and provenance. It extends over an area of about 420 m2, with a 20.25x20.40m squared plan and an overall height of 19.50m, on three floors.

Figure 9. The inner courtyard.

Field tests have been performed to identify its dynamic characteristics with the purpose of the calibration of a numerical model for future evaluation of the structural health in order to preserve the historical and architectural uniqueness of the building in a relevant seismic area as Palermo (Bilello et al. 2016).

3.1 Acquisition of the structural response signals

As far as the first step of the procedure is concerned, the acceleration measurements have been acquired using eight high-sensitivity piezoelectric mono-axial accelerometers, whose

characteristics are listed in Table 3. Four couples of the overall eight accelerometers have been located at four measuring points to record bi-axial accelerations, along the u_1 and u_2 directions, respectively. Accelerometers n°1-4 have been oriented along the u_1 axis while n°5-8 along the u_2 axis. The couple {n°1, n°5} has been placed at the ground floor, the another one, {n°2,n°6}, at the first floor and the two couples {n°3, n°7} and {n°4, n°8} at the second floor of the courtyard (Figure 10).

Table 3. Accelerometers features.

Feature	Value
Sensitivity	1000 mV/g
Measuring range	±5 g pk
Frequency range	0.06 to 450 Hz
Broadband Resolution	0.000003 g rms
Mass	50 grams

Six tests have been performed considering an observation window of ten minutes and acceleration data have been recorded by sensors using a sampling frequency of 100 Hz. Further details of the experimental setup are reported in references (Bilello et al. 2016). Data in the following are referred to one test within the six tests since no significant variations have been found.

The structural recorded accelerations $\ddot{x}_j(t)$ (with $j=1,2,...,N$), being N=8 the number of recording channels, are assumed to be stationary and ergodic random processes, outputs of a linear system excited by white noise input.

The identification of modal parameters starts from the evaluation of the auto Power Spectral Density (PSD) and Cross-Power Spectral Density (CPSD) functions associated to the acquired data.

It is worth noting that the case study, here taken into account, represents a MDOF system so the initial PSD matrix of the response data contains multicomponent PSDs and CPSDs characterized by the contribution of all the modes for each channel.

As a consequence, after the PSD matrix estimation with the Welch Method, its decomposition into monocomponent PSDs/CPSDs, in order to estimate the correspondent filtered correlation functions.

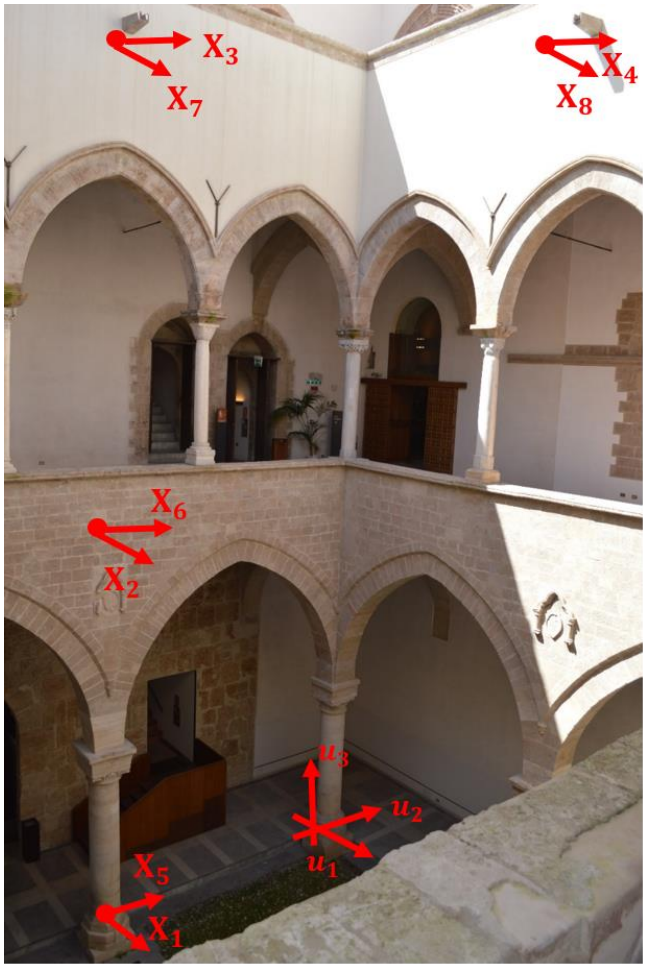

Figure 10. Location of measuring points and sensor labelling.

3.2 *Estimation of the PSDs from output data*

The PSD matrix is obtained using Welch's method which subdivides each acceleration $\ddot{x}_j(t)$ into $\bar{N}$ sub-signals and computes a modified periodogram for each segment. As in the SDOF case, the segments are typically multiplied by a window function and overlapped in time to avoid information loss at the beginning and end of each segment. In this study a length of the sub-segments of 40.95 sec (4096 sampling points), a Hamming function for windowing and a 50% overlap between adjacent segments have been assumed.

In view of the above, the two-sided PSDs $S_{\ddot{x}_j\ddot{x}_k,r}(f)$ (with $k=1,2,...,N$) for each sub-segments can be obtained by:

$$S_{\ddot{x}_j\ddot{x}_k,r}(f)=\frac{1}{2\pi}lim_{T\to\infty}\frac{1}{2T}E[X_{j,r}(f)X_{k,r}(f)^*] \tag{18}$$

where * denotes the conjugate transpose and $X_{j,r}(f)$ is the Fourier transform of the sub-signal $\ddot{x}_j(t)$. Specifically, when $k=j$ the PSDs

$S_{\ddot{x}_j\ddot{x}_j,r}(f)$ are obtained, while if $k \neq j$, $S_{\ddot{x}_j\ddot{x}_k,r}(f)$ represent the CPSDs of the system.

Then, considering the mean of all the contributes, the final PSDs and CPSDs are obtained by:

$$S_{\ddot{x}_j\ddot{x}_k}(f) = \frac{1}{\bar{N}} \sum_{r=1}^{\bar{N}} S_{\ddot{x}_j\ddot{x}_k,r}(f) \tag{19}$$

Thus, the PSDs $S_{\ddot{x}_j\ddot{x}_j}(f)$ and the cross ones $S_{\ddot{x}_j\ddot{x}_k}(f)$ are collected in the two-sided PSD matrix $\boldsymbol{S}_{\ddot{x}\ddot{x}}(f)$, as diagonal and off-diagonal terms respectively, as follows:

$$\boldsymbol{S}_{\ddot{x}\ddot{x}}(f) = \begin{bmatrix} S_{\ddot{x}_1\ddot{x}_1}(f) & S_{\ddot{x}_1\ddot{x}_2}(f) & \dots & S_{\ddot{x}_1\ddot{x}_N}(f) \\ S_{\ddot{x}_2\ddot{x}_1}(f) & S_{\ddot{x}_2\ddot{x}_2}(f) & \dots & S_{\ddot{x}_2\ddot{x}_N}(f) \\ \dots & \dots & \dots & \dots \\ S_{\ddot{x}_N\ddot{x}_1}(f) & S_{\ddot{x}_N\ddot{x}_2}(f) & \dots & S_{\ddot{x}_N\ddot{x}_N}(f) \end{bmatrix}$$

It is worth stressing that each term of $\boldsymbol{S}_{\ddot{x}\ddot{x}}(f)$, obtained by the use of the Welch Method, is a multicomponent function.

Figure 11-12 show auto PSDs functions $S_{\ddot{x}_j\ddot{x}_j}(f)$ obtained from the acquired accelerations for channels 1-4 (u_1-axis) and 5-8 (u_2-axis). It can be clearly pointed out the presence of structural modes in the frequency range 0-6 Hz. Furthermore, it should be also noticed that, in the frequency range between 3.0 Hz and 4.2 Hz, PSDs exhibit a series of local maxima representing possible multiple modes closely spaced.

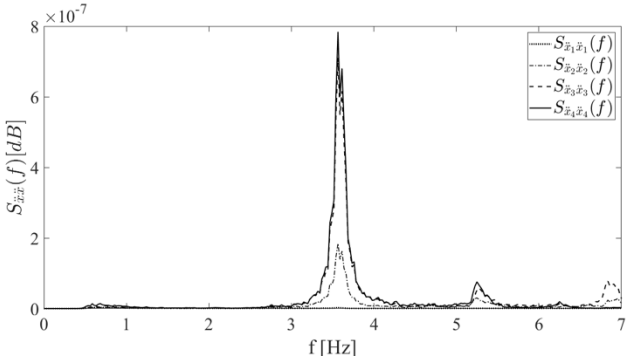

Figure 11. PSDs of acquired signals: channels 1-4 u1-axis.

At this stage, many ambient identification methods, such as the PP+HP and FDD, determine all the modal characteristics considering the multicomponent PSDs/CPSDs and their phases.

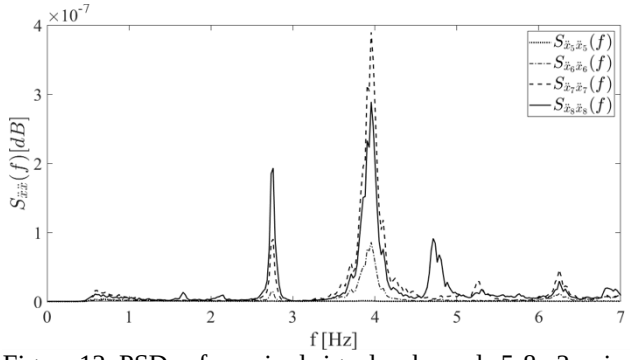

Figure 12. PSDs of acquired signals: channels 5-8 u2-axis.

Firstly, in this study, natural frequencies and damping coefficients of the structure have been estimated directly from the peaks of the PSDs using the PP+HP method (Barbé 2010).

Table 4 lists the first four identified natural frequencies and the corresponding damping ratios. Frequencies can be considered accurate enough since the deviation from different data sets was very small, while damping ratios appear to be lower than expected for masonry buildings; however, the structure has been investigated in operational conditions and this is consistent with the fact that the energy dissipation associated to micro-tremors is usually much smaller than during strong excitation as earthquakes.

Table 4. Estimated natural frequencies and damping ratios with the PP+HP method.

Mode n°	$\bar{f}$ [Hz]	ξ [%]
1	2.7554	1.3291
2	3.5645	2.0548
3	3.9551	2.2226
4	5.2576	1.8819

Thus, considering the well-attained estimation of the damping ratio for the SDOF system analysed in Section 2, the ASM is focused on a more accurate definition of the damping. To this end, it suggests operating on filtered signals (FPSDs/FCPSDs) and to derive the frequencies and damping ratios from the analytical signals expressed in terms of FCORs/FCCORs in the time domain.

In this regard, to decompose multicomponent signals many kinds of filters exist in literature: Butterworth, Elliptic or Chebyshev and so on, with different specifications (Van Valkenburg 1982). In order to isolate the contribution of each mode, the use of filters requires the definition of a frequency range centered on the frequency of the analyzed mode. However, frequencies can be easily obtained by an initial use of the PP method. In this case a Butterworth band-pass filter of order 8 has been considered.

Once the Butterworth filter has been applied to each multicomponent PSD (auto and cross) of the original PSD matrix, as many FPSDs and FCPSDs as the number of channels are obtained for each mode, each one containing characteristics of only one individual mode.

Thus, applying the filter to the original multicomponent $S_{\ddot{x}_1\ddot{x}_1}(f)$ for instance, in the frequency range centered on the first frequency of the system (2.62-2.89 Hz), a FPSD, denoted as ${}_F S_{\ddot{x}_1\ddot{x}_1}(f)$, characterized by the contribution of the first mode only, is obtained.
Repeating the same procedure for each original PSD $S_{\ddot{x}_j\ddot{x}_j}(f)$, eight FPSDs ${}_F S_{\ddot{x}_j\ddot{x}_j}(f)$ are obtained in total for the first mode.

In Figure 13 the four functions ${}_F S_{\ddot{x}_j\ddot{x}_j}(f)$ of acceleration responses, only recorded along the u_1 axis, are depicted. They represent the PSDs of four single oscillators dominated by the modal parameters of the first mode only. As emerges, all the peaks comparing in Figure 11 are not visible anymore and only the first mode can be clearly individuated.

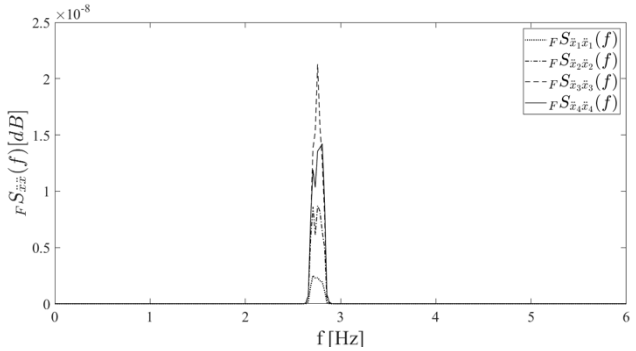

Figure 13: FPSDs of the structural acceleration responses (recorded along the u1 axis) in correspondence of the first mode.

In the same way, filtering the original CPSDs $S_{\ddot{x}_j\ddot{x}_k}(f)$, corresponding FCPSDs ${}_F S_{\ddot{x}_j\ddot{x}_k}(f)$ are obtained for the first mode.

Changing the frequency range of the filter to correspond with the next modes FPSDs and the FCPSDs are obtained for the other modes too. In Figure 14 the four functions ${}_F S_{\ddot{x}_j\ddot{x}_j}(f)$ of acceleration responses only recorded along the u_1 axis are depicted considering this time the filtering in the frequency range of the second mode (3.38-3.74Hz). As can be seen, the contribute of the first mode, highlighted in Figure 14) by the peak in the range 2.62-2.89 Hz, is disappeared as well as all the other modes except from the second one.

In this manner, henceforward the modal analysis for each signal is the same as that described in the SDOF case. Clearly, for a SDOF structure, the solution of the modal parameters is unique, while for a MDOF system, the mean of the values obtained for each channel should be considered.

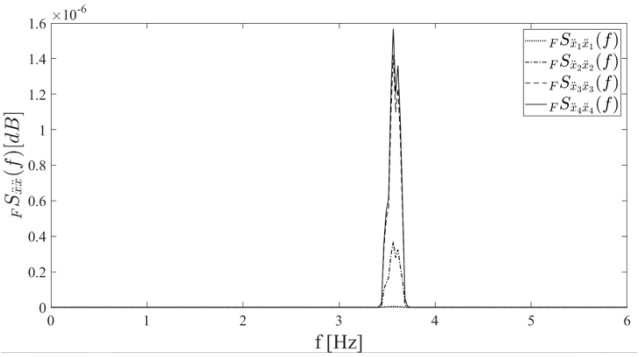

Figure 14: FPSDs of the structural acceleration responses (recorded along the u1 axis) in correspondence of the second mode.

3.3 Estimation of the CORs from the PSDs

Then, by means of the IFFT, from the obtained FPSDs/FCPSDs, the estimation of the FCORs/FCCORs follows. Obviously, the procedure should be repeated for all the channels and for all the number of modes of interest.

In Figures 15-16 the FCORs, denoted as ${}_F R_{\ddot{x}_j\ddot{x}_j}(f)$ of the signals recorded along the u_1 axis are shown. Figure 15 shows the four functions ${}_F R_{\ddot{x}_j\ddot{x}_j}(f)$ filtered in correspondence of the first mode while Figure 16 in correspondence of the second one.

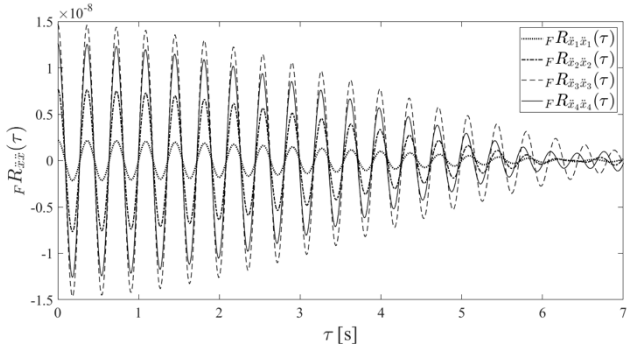

Figure 15: FCORs of the structural acceleration responses (recorded along the u1 axis) filtered in correspondence of the first mode.

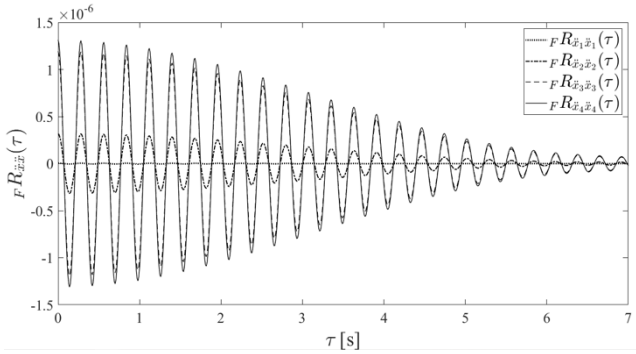

Figure 16: FCORs of the structural acceleration responses (recorded along the u1 axis) filtered in correspondence of the second mode.

3.4 Estimation of the AS and its properties

Finally, by applying the Hilbert transform to the FCORs/FCCORs, filtered analytical signal are derived too and the same procedure shown for the SDOF case can be carried out.

3.5 Identification of the modal parameters

Table 5 shows results derived from the application of the ASM for the first four modes and discrepancies have been computed assuming the PP+HP method as reference.

As shown, using the proposed approach, the identified frequencies and damping ratios are almost identical to those estimated by the PP+HP (Table 4).

Table 5: Estimated natural frequencies and damping ratios with the ASM.

Mode n°	$\overline{f}$ [Hz]	Discrepancy [%]	ξ [%]	Discrepancy [%]
1	2.7452	0.3548	1.17	11.6947
2	3.5883	0.6821	1.42	30.9794
3	3.9395	0.3907	1.52	31.7027
4	4.7212	0.0466	1.58	13.0246

Clearly, dealing with an existing historic building, do not exist any exact theoretical values as reference in order to establish the accuracy among the several identification methods.

Nevertheless, close values of modal parameters, obtained through different procedures, suggest the reliability of the proposed technique. Indeed, the estimation of the modal parameters based on the proposed procedure is in agreement with the traditional PP+HP method, especially in terms of frequencies.

More differences are achieved in the definition of damping coefficients. However, since the analytical signal is more sensitive to changes of structural characteristics over time, the extraction of modal parameters by the instantaneous frequency and amplitude associated with the monocomponent correlation functions, may be particularly efficient in the field of structural monitoring.

4 CONCLUSION

In this paper, a novel identification procedure from ambient vibration data, denoted as Analytical Signal-based method (ASM), is proposed for the estimation of the modal parameters of a structure under the white noise assumption as input force.

The method is based on the use of the Analytical Signal and the Hilbert Transform, applied to properly decomposed response data. Indeed, when a MDOF system is considered, the structural responses are characterized by the influence of all the structural modes and the modal parameters cannot be extracted directly from them in the time domain, so they need to be decomposed. The decomposition of the output signal, by means of the Butterworth filter, leads to a set of monocomponent signals corresponding to several SDOF systems, each one containing information about a specific structural mode. The presented approach requires only the frequencies of the modes which can be easily detected by the Peak Picking method.

As shown, natural frequencies and damping ratios can be obtained from the analytical signal of the estimated filtered correlation functions, which in turn have been achieved from the filtered power spectral density functions of the output signal.

In order to investigate the reliability of this approach to extract dynamic characteristics of structures of the cultural heritage, ambient vibration tests have been performed on the Chiarmonte-Steri Palace, an historical building located in Palermo. Specifically, the ASM has been applied to recorded signals of eight accelerometers opportunely located in the inner courtyard of the structure.

Results derived by the use of ASM, compared to the classical PP+HP, suggest that the proposed approach can be considered as a reliable output-only technique for frequencies and damping ratios extraction from the analytical signal.

On the basis of the encouraging results, future research will aimed at investigating the reliability of the ASM to detect the mode shapes so that the overall dynamic behavior of the system can be detected.

REFERENCES

Agneni A., 2004. On Modal Parameter Estimates from Ambient Vibration Tests. *Proceedings of the*

International Conference on Noise and Vibration Engineering: ISMA2004, Leuven, Belgium.

Barone G., Marino F. and Pirrotta A., 2008. Low stiffness variation in structural systems: identification and localization, *Structural Control and Health Monitoring*, **15**, 450-470.

Barbé K., Pintelon R., Schoukens J., 2010. Welch Method Revisited: Nonparametric Power Spectrum Estimation Via Circular Overlap, *IEEE Trans. Signal Processing*, 58, 47-78.

Bedrosian E., 1962. The analytic signal representation of modulated waveforms, *Proc IRE*, **50**, 10, 2071-2076.

Bedrosian E., 1963. A product theorem for Hilbert transform, *Proc IEEE*, **51**, 5, 868-869.

Bendat J. S. and Piersol A. G., 1993. *Engineering Applications of Correlation and Spectral Analysis*, John Wiley & Sons.

Bendat J. S and Piersol A. G., 2011. *Random Data: Analysis and Measurement Procedures*, John Wiley and Sons, Hoboken.

Bilello C., Greco E., Greco M., Madonia N., Pirrotta A. and Sorce A., 2016. A Numerical Model for Pre-Monitoring Design of Historical Colonnade Courtyards: The Case Study of Chiaramonte Palace in Palermo, *The Open Construction and Building Technology Journal*, **10**, (Suppl 1: M3), 52-64.

Brincker R., Zhang L. and Andersen P., 2000. Modal Identification from Ambient Responses using Frequency Doman Decomposition, *in Proc. of the International Modal Analysis Conference (IMAC)*, San Antonio, Texas.

Brincker R., Zhang L. and Andersen P., 2000. Output- Only Modal Analysis by Frequency Domain Decomposition, *in Proc. of the ISMA25 conference in Leuvcn*.

Brincker R., Zhang L., Andersen P., 2005. An Overview of Operational Modal Analysis: Major Development and Issues, *Proceedings of the 1st International Operational Modal Analysis Conference*, Copenhagen, Denmark.

Cottone G., Pirrotta A. and Salamone S., 2008. Incipient Damage Identification through Characteristics of the Analytical Signal Response, *Structural Control and Health Monitoring*, **15**, 1122-1142.

Cottone G., Fileccia Scimemi G., Pirrotta A., 2014. α-stable distributions for better performance of ACO in detecting damage on not well spaced frequency systems, *Probabilistic Engineering Mechanics*, **35**, pp.29-36.

Giuffrè M., Pezzini E., Sciascia L., 2008. *Consulenza storico-architettonica per il progetto di recupero del complesso monumentale dello Steri*, Università degli Studi di Palermo.

Lima A.I., 2006. *Lo Steri di Palermo nel secondo Novecento - dagli studi di Giuseppe Spatrisano al progetto di Roberto Calandra con la consulenza di Carlo Scarpa*, Dario Flaccovio Editore, Palermo.

Lo Iacono F., Navarra G. and Pirrotta A., 2012. A Damage Identification procedure based on Hilbert transform: experimental validation, *Structural Control and Health Monitoring*, **19**, 146-160.

Van Valkenburg M.E., 1982. *Analog Filter Design*, Holt-Saunders International Edition.

Welch P. D., 1967. The use of fast fourier transform for the estimation of power spectra: a method based on time averaging over short, modified periodograms, *IEEE Trans. Audio Electroacoust*..